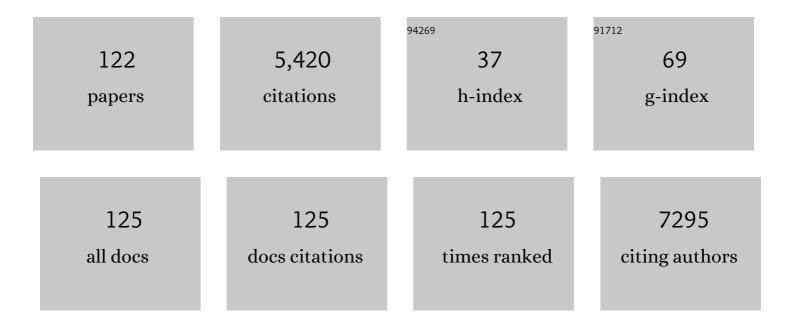
Gary A Ulaner

List of Publications by Year in descending order

Source: https://exaly.com/author-pdf/6201299/publications.pdf Version: 2024-02-01



CARY A LILANER

#	Article	IF	CITATIONS
1	HER kinase inhibition in patients with HER2- and HER3-mutant cancers. Nature, 2018, 554, 189-194.	13.7	572
2	Ado-Trastuzumab Emtansine for Patients With <i>HER2</i> -Mutant Lung Cancers: Results From a Phase II Basket Trial. Journal of Clinical Oncology, 2018, 36, 2532-2537.	0.8	381
3	Vemurafenib for <i>BRAF</i> V600–Mutant Erdheim-Chester Disease and Langerhans Cell Histiocytosis. JAMA Oncology, 2018, 4, 384.	3.4	280
4	Efficacy of MEK inhibition in patients with histiocytic neoplasms. Nature, 2019, 567, 521-524.	13.7	222
5	IVF results in de novo DNA methylation and histone methylation at an Igf2-H19 imprinting epigenetic switch. Molecular Human Reproduction, 2005, 11, 631-640.	1.3	164
6	HER2-Mediated Internalization of Cytotoxic Agents in <i>ERBB2</i> Amplified or Mutant Lung Cancers. Cancer Discovery, 2020, 10, 674-687.	7.7	149
7	Detection of HER2-Positive Metastases in Patients with HER2-Negative Primary Breast Cancer Using ⁸⁹ Zr-Trastuzumab PET/CT. Journal of Nuclear Medicine, 2016, 57, 1523-1528.	2.8	146
8	Absence of a telomere maintenance mechanism as a favorable prognostic factor in patients with osteosarcoma. Cancer Research, 2003, 63, 1759-63.	0.4	136
9	Loss of imprinting of IGF2 and H19 in osteosarcoma is accompanied by reciprocal methylation changes of a CTCF-binding site. Human Molecular Genetics, 2003, 12, 535-549.	1.4	132
10	First-in-Human Human Epidermal Growth Factor Receptor 2–Targeted Imaging Using ⁸⁹ Zr-Pertuzumab PET/CT: Dosimetry and Clinical Application in Patients with Breast Cancer. Journal of Nuclear Medicine, 2018, 59, 900-906.	2.8	126
11	Activating mutations in CSF1R and additional receptor tyrosine kinases in histiocytic neoplasms. Nature Medicine, 2019, 25, 1839-1842.	15.2	122
12	Prognostic value of FDC-PET prior to autologous stem cell transplantation for relapsed and refractory diffuse large B-cell lymphoma. Blood, 2015, 125, 2579-2581.	0.6	111
13	Molecular Classification of Breast Cancer. PET Clinics, 2018, 13, 325-338.	1.5	103
14	High prevalence of myeloid neoplasms in adults with non–Langerhans cell histiocytosis. Blood, 2017, 130, 1007-1013.	0.6	98
15	Comparison of ¹⁸ F-FDG PET/CT for Systemic Staging of Newly Diagnosed Invasive Lobular Carcinoma Versus Invasive Ductal Carcinoma. Journal of Nuclear Medicine, 2015, 56, 1674-1680.	2.8	92
16	Retrospective Analysis of ¹⁸ F-FDG PET/CT for Staging Asymptomatic Breast Cancer Patients Younger Than 40 Years. Journal of Nuclear Medicine, 2014, 55, 1578-1583.	2.8	87
17	Divergent patterns of telomere maintenance mechanisms among human sarcomas: Sharply contrasting prevalence of the alternative lengthening of telomeres mechanism in Ewing's sarcomas and osteosarcomas. Genes Chromosomes and Cancer, 2004, 41, 155-162.	1.5	85
18	Efficacy and Determinants of Response to HER Kinase Inhibition in <i>HER2</i> -Mutant Metastatic Breast Cancer. Cancer Discovery, 2020, 10, 198-213.	7.7	83

#	Article	IF	CITATIONS
19	89Zr-Trastuzumab PET/CT for Detection of Human Epidermal Growth Factor Receptor 2–Positive Metastases in Patients With Human Epidermal Growth Factor Receptor 2–Negative Primary Breast Cancer. Clinical Nuclear Medicine, 2017, 42, 912-917.	0.7	81
20	Appearance of untreated bone metastases from breast cancer on FDG PET/CT: importance of histologic subtype. European Journal of Nuclear Medicine and Molecular Imaging, 2015, 42, 1666-1673.	3.3	79
21	PET/CT for Patients With Breast Cancer: Where Is the Clinical Impact?. American Journal of Roentgenology, 2019, 213, 254-265.	1.0	78
22	Identifying and Distinguishing Treatment Effects and Complications from Malignancy at FDG PET/CT. Radiographics, 2013, 33, 1817-1834.	1.4	75
23	Comparison of FDC-PET/CT and contrast-enhanced CT for monitoring therapy response in patients with metastatic breast cancer. European Journal of Nuclear Medicine and Molecular Imaging, 2017, 44, 1428-1437.	3.3	74
24	CD38-targeted Immuno-PET of Multiple Myeloma: From Xenograft Models to First-in-Human Imaging. Radiology, 2020, 295, 606-615.	3.6	73
25	A prospective trial of dynamic contrast-enhanced MRI perfusion and fluorine-18 FDG PET-CT in differentiating brain tumor progression from radiation injury after cranial irradiation. Neuro-Oncology, 2016, 18, 873-880.	0.6	72
26	Head-to-Head Evaluation of ¹⁸ F-FES and ¹⁸ F-FDG PET/CT in Metastatic Invasive Lobular Breast Cancer. Journal of Nuclear Medicine, 2021, 62, 326-331.	2.8	69
27	18F-Fluoroestradiol PET/CT Measurement of Estrogen Receptor Suppression during a Phase I Trial of the Novel Estrogen Receptor-Targeted Therapeutic GDC-0810: Using an Imaging Biomarker to Guide Drug Dosage in Subsequent Trials. Clinical Cancer Research, 2017, 23, 3053-3060.	3.2	66
28	Initial Results of a Prospective Clinical Trial of ¹⁸ F-Fluciclovine PET/CT in Newly Diagnosed Invasive Ductal and Invasive Lobular Breast Cancers. Journal of Nuclear Medicine, 2016, 57, 1350-1356.	2.8	60
29	Molecular Imaging of Biomarkers in Breast Cancer. Journal of Nuclear Medicine, 2016, 57, 53S-59S.	2.8	56
30	Standardized uptake value by positron emission tomography/computed tomography as a prognostic variable in metastatic breast cancer. Cancer, 2012, 118, 5454-5462.	2.0	55
31	Prognostic value of quantitative fluorodeoxyglucose measurements in newly diagnosed metastatic breast cancer. Cancer Medicine, 2013, 2, 725-733.	1.3	54
32	18F-FDG-PET/CT for systemic staging of newly diagnosed triple-negative breast cancer. European Journal of Nuclear Medicine and Molecular Imaging, 2016, 43, 1937-1944.	3.3	53
33	Human Epidermal Growth Factor Receptor 2-Targeted PET/Single- Photon Emission Computed Tomography Imaging of Breast Cancer. PET Clinics, 2017, 12, 269-288.	1.5	49
34	CD8-targeted PET Imaging of Tumor Infiltrating T cells in Patients with Cancer: A Phase I First-in-Human Study of ⁸⁹ Zr-Df-IAB22M2C, a Radiolabeled anti-CD8 Minibody. Journal of Nuclear Medicine, 2021, , jnumed.121.262485.	2.8	49
35	Metabolic tumor volume and total lesion glycolysis on FDG-PET/CT can predict overall survival after 90Y radioembolization of colorectal liver metastases: A comparison with SUVmax, SUVpeak, and RECIST 1.0. European Journal of Radiology, 2016, 85, 1224-1231.	1.2	47
36	Prospective Clinical Trial of ¹⁸ F-Fluciclovine PET/CT for Determining the Response to Neoadjuvant Therapy in Invasive Ductal and Invasive Lobular Breast Cancers. Journal of Nuclear Medicine, 2017, 58, 1037-1042.	2.8	47

#	Article	IF	CITATIONS
37	Accelerated single cell seeding in relapsed multiple myeloma. Nature Communications, 2020, 11, 3617.	5.8	41
38	18F–FDG-PET/CT for systemic staging of patients with newly diagnosed ER-positive and HER2-positive breast cancer. European Journal of Nuclear Medicine and Molecular Imaging, 2017, 44, 1420-1427.	3.3	40
39	Single-agent dabrafenib for <i>BRAF</i> ^{V600E} -mutated histiocytosis. Haematologica, 2018, 103, e177-e180.	1.7	40
40	ACR Appropriateness Criteria® Evaluation of theÂSymptomatic Male Breast. Journal of the American College of Radiology, 2018, 15, S313-S320.	0.9	40
41	Identification of HER2-Positive Metastases in Patients with HER2-Negative Primary Breast Cancer by Using HER2-targeted ⁸⁹ Zr-Pertuzumab PET/CT. Radiology, 2020, 296, 370-378.	3.6	40
42	Epigenetic regulation oflgf2/H19 imprinting at CTCF insulator binding sites. Journal of Cellular Biochemistry, 2003, 90, 1038-1055.	1.2	36
43	Detection of Internal Mammary Adenopathy in Patients With Breast Cancer by PET/CT and MRI. American Journal of Roentgenology, 2015, 205, 899-904.	1.0	31
44	Factors Affecting Oncologic Outcomes of 90Y Radioembolization of Heavily Pre-Treated Patients With Colon Cancer Liver Metastases. Clinical Colorectal Cancer, 2019, 18, 8-18.	1.0	31
45	The Influence of Glycans-Specific Bioconjugation on the FcγRI Binding and <i>In vivo</i> Performance of ⁸⁹ Zr-DFO-Pertuzumab. Theranostics, 2020, 10, 1746-1757.	4.6	31
46	Neurologic and oncologic features of Erdheim–Chester disease: a 30-patient series. Neuro-Oncology, 2020, 22, 979-992.	0.6	31
47	Epigenetic regulation of the taxol resistance–associated gene TRAG-3 in human tumors. Cancer Genetics and Cytogenetics, 2004, 151, 1-13.	1.0	30
48	Is Methylene Diphosphonate Bone Scan Necessary for Initial Staging of Ewing Sarcoma if ¹⁸ F-FDG PET/CT Is Performed?. American Journal of Roentgenology, 2014, 202, 859-867.	1.0	30
49	Ipilimumab-Induced Colitis on FDG PET/CT. Clinical Nuclear Medicine, 2012, 37, 629-630.	0.7	29
50	B-Cell Non-Hodgkin Lymphoma: PET/CT Evaluation after ⁹⁰ Y–lbritumomab Tiuxetan Radioimmunotherapy—Initial Experience ¹ . Radiology, 2008, 246, 895-902.	3.6	28
51	Comparison of the effectiveness of MRI perfusion and fluorine-18 FDG PET-CT for differentiating radiation injury from viable brain tumor: a preliminary retrospective analysis with pathologic correlation in all patients. Clinical Imaging, 2013, 37, 451-457.	0.8	28
52	Prognostic value of FDG PET/CT-based metabolic tumor volumes in metastatic triple negative breast cancer patients. American Journal of Nuclear Medicine and Molecular Imaging, 2016, 6, 120-7.	1.0	28
53	The Impact That Number of Analyzed Metastatic Breast Cancer Lesions Has on Response Assessment by ¹⁸ F-FDG PET/CT Using PERCIST. Journal of Nuclear Medicine, 2016, 57, 1102-1104.	2.8	26
54	Trends in oncologic hybrid imaging. European Journal of Hybrid Imaging, 2018, 2, 1.	0.6	25

#	Article	IF	CITATIONS
55	Dual PET Imaging in Bronchial Neuroendocrine Neoplasms: The NETPET Score as a Prognostic Biomarker. Journal of Nuclear Medicine, 2021, 62, 1278-1284.	2.8	25
56	Activating and silencing histone modifications form independent allelic switch regions in the imprinted Gnas gene. Human Molecular Genetics, 2004, 13, 741-750.	1.4	24
57	AMEERA-1 phase 1/2 study of amcenestrant, SAR439859, in postmenopausal women with ER-positive/HER2-negative advanced breast cancer. Nature Communications, 2022, 13, .	5.8	24
58	Telomere maintenance in clinical medicine. American Journal of Medicine, 2004, 117, 262-269.	0.6	23
59	Prognostic Value of FDG PET/CT before Allogeneic and Autologous Stem Cell Transplantation for Aggressive Lymphoma. Radiology, 2015, 277, 518-526.	3.6	23
60	False-Positive [¹⁸ F]Fluorodeoxyglucose-Avid Lymph Nodes on Positron Emission Tomography–Computed Tomography After Allogeneic but Not Autologous Stem-Cell Transplantation in Patients With Lymphoma. Journal of Clinical Oncology, 2014, 32, 51-56.	0.8	22
61	Rosai-Dorfman Disease—Utility of 18F-FDG PET/CT for Initial Evaluation and Follow-up. Clinical Nuclear Medicine, 2020, 45, e260-e266.	0.7	22
62	Clinical Potential of Human Epidermal Growth Factor Receptor 2 and Human Epidermal Growth Factor Receptor 3 Imaging in Breast Cancer. PET Clinics, 2018, 13, 423-435.	1.5	21
63	16α-18F-fluoro-17β-Fluoroestradiol (FES): Clinical Applications for Patients With Breast Cancer. Seminars in Nuclear Medicine, 2022, 52, 574-583.	2.5	19
64	Amino Acid Metabolism as a Target for Breast Cancer Imaging. PET Clinics, 2018, 13, 437-444.	1.5	18
65	Focal Immunotherapy-Induced Pancreatitis Mimicking Metastasis on FDG PET/CT. Clinical Nuclear Medicine, 2019, 44, 836-837.	0.7	18
66	Defining the undetectable: The current landscape of minimal residual disease assessment in multiple myeloma and goals for future clarity. Blood Reviews, 2021, 46, 100732.	2.8	18
67	FDG PET/CT Assesses the Risk of Femoral Pathological Fractures in Patients With Metastatic Breast Cancer. Clinical Nuclear Medicine, 2017, 42, 264-270.	0.7	16
68	ACR Appropriateness Criteria® Stage I Breast Cancer: Initial Workup and Surveillance for Local Recurrence and Distant Metastases in Asymptomatic Women. Journal of the American College of Radiology, 2019, 16, S428-S439.	0.9	16
69	Breast Implant Foreign Body Reaction Mimicking Breast Cancer Recurrence on FDG PET/CT. Clinical Nuclear Medicine, 2013, 38, 480-481.	0.7	15
70	Diagnostic Role of Fluorodeoxyglucose PET in Breast Cancer. PET Clinics, 2018, 13, 355-361.	1.5	15
71	Diffusion and Perfusion MRI Predicts Response Preceding and Shortly After Radiosurgery to Brain Metastases: A Pilot Study. Journal of Neuroimaging, 2021, 31, 317-323.	1.0	14
72	Impact of FDG PET Imaging for Expanding Patient Eligibility and Measuring Treatment Response in a Genome-Driven Basket Trial of the Pan-HER Kinase Inhibitor, Neratinib. Clinical Cancer Research, 2019, 25, 7381-7387.	3.2	13

#	Article	IF	CITATIONS
73	Mars Shot for Nuclear Medicine, Molecular Imaging, and Molecularly Targeted Radiopharmaceutical Therapy. Journal of Nuclear Medicine, 2021, 62, 6-14.	2.8	13
74	Visualization of telomerase reverse transcriptase (hTERT) promoter activity using a trimodality fusion reporter construct. Journal of Nuclear Medicine, 2006, 47, 270-7.	2.8	13
75	Phase II Trial of Imatinib Plus Binimetinib in Patients With Treatment-Naive Advanced Gastrointestinal Stromal Tumor. Journal of Clinical Oncology, 2022, 40, 997-1008.	0.8	13
76	Value of second-opinion review of outside institution PET-CT examinations. Nuclear Medicine Communications, 2017, 38, 306-311.	0.5	12
77	¹⁸ F-FDG PET/CT for Systemic Staging of Newly Diagnosed Breast Cancer in Men. Journal of Nuclear Medicine, 2019, 60, 472-477.	2.8	11
78	Detection of recurrent pancreatic cancer: value of second-opinion interpretations of cross-sectional images by subspecialized radiologists. Abdominal Radiology, 2019, 44, 586-592.	1.0	11
79	Musculoskeletal tumors and tumor-like conditions: common and avoidable pitfalls at imaging in patients with known or suspected cancer. International Orthopaedics, 2013, 37, 871-876.	0.9	10
80	18F-FDG PET/CT versus anatomic imaging for evaluating disease extent and clinical trial eligibility in Erdheim-Chester disease: results from 50 patients in a registry study. European Journal of Nuclear Medicine and Molecular Imaging, 2021, 48, 1154-1165.	3.3	10
81	Long–Half-Life ⁸⁹ Zr-Labeled Radiotracers Can Guide Percutaneous Biopsy Within the PET/CT Suite Without Reinjection of Radiotracer. Journal of Nuclear Medicine, 2018, 59, 399-402.	2.8	9
82	Current and potential applications of positron emission tomography for multiple myeloma and plasma cell disorders. Best Practice and Research in Clinical Haematology, 2020, 33, 101148.	0.7	9
83	Musculoskeletal tumours and tumour-like conditions: common and avoidable pitfalls at imaging in patients with known or suspected cancer. International Orthopaedics, 2013, 37, 877-882.	0.9	8
84	FDG PET/CT Findings in a Rare Case of Giant Fibrovascular Polyp of the Esophagus Harboring Atypical Lipomatous Tumor/Well-Differentiated Liposarcoma. Clinical Nuclear Medicine, 2014, 39, 288-291.	0.7	8
85	False-Positive FDG PET/CT Due to Liver Parenchymal Injury Caused By a Surgical Retractor. Clinical Nuclear Medicine, 2012, 37, 910-911.	0.7	7
86	Pathologically Benign Lymph Nodes Can Mimic Malignancy on Imaging in Patients With Angiomatoid Fibrous Histiocytoma. Clinical Orthopaedics and Related Research, 2017, 475, 2274-2279.	0.7	7
87	Efficacy and Safety of Gemcitabine With Trastuzumab and Pertuzumab After Prior Pertuzumab-Based Therapy Among Patients With Human Epidermal Growth Factor Receptor 2–Positive Metastatic Breast Cancer. JAMA Network Open, 2019, 2, e1916211.	2.8	7
88	Clinical Utility of ¹⁸ F-FDG PET/CT for Staging and Treatment Planning in Urachal Adenocarcinoma. Journal of Nuclear Medicine, 2021, 62, 643-647.	2.8	7
89	Improved image reconstruction of 89Zr-immunoPET studies using a Bayesian penalized likelihood reconstruction algorithm. EJNMMI Physics, 2021, 8, 6.	1.3	7
90	Highâ€resolution and highâ€sensitivity PET for quantitative molecular imaging of the monoaminergic nuclei: A GATE simulation study. Medical Physics, 2022, 49, 4430-4444.	1.6	7

#	Article	IF	CITATIONS
91	Predictive Value of Positron Emission Tomography/Computed Tomography to Assess Early Treatment Response to Dual Human Epidermal Growth Factor Receptor 2 (HER2) Blockade Without Chemotherapy for HER2-Positive Metastatic Breast Cancer: Are We Ready to Embrace This "Early Metabolic Look― Strategy?. Journal of Clinical Oncology, 2015, 33, 2591-2593.	0.8	6
92	Hepatocellular Carcinoma Mimicking Neuroendocrine Tumor Metastasis on 68Ga-DOTATATE PET/CT. Clinical Nuclear Medicine, 2019, 44, 330-331.	0.7	6
93	FDG PET/CT Demonstration of Right Atrium Metastasis Overlooked on Contrast-Enhanced CT. Clinical Nuclear Medicine, 2011, 36, 405-406.	0.7	5
94	Unilateral Suppression of Brown Fat on FDG PET/CT in Horner Syndrome. Clinical Nuclear Medicine, 2016, 41, 797-798.	0.7	5
95	Specialized second-opinion radiology review of PET/CT examinations for patients with diffuse large B-cell lymphoma impacts patient care and management. Medicine (United States), 2017, 96, e9411.	0.4	5
96	The Contribution of MicroRNAs to the Inflammatory and Neoplastic Characteristics of Erdheim–Chester Disease. Cancers, 2020, 12, 3240.	1.7	5
97	Vemurafenib in Patients with Erdheim-Chester Disease (ECD) and Langerhans Cell Histiocytosis (LCH) Harboring BRAFV600 Mutations: A Cohort of the Histology-Independent VE-Basket Study. Blood, 2016, 128, 480-480.	0.6	5
98	Mucinous urachal adenocarcinoma: A potential nonfluorodeoxyglucose-avid pitfall on 18fluorine-fluorodeoxyglucose positron emission tomography/computed tomography. World Journal of Nuclear Medicine, 2020, 19, 432-434.	0.3	5
99	Uses and Opportunities for Molecular Imaging in Patients with Breast Cancer. PET Clinics, 2018, 13, xi-xii.	1.5	4
100	Evidence-Based Best Practices. Clinical Nuclear Medicine, 2021, 46, 569-570.	0.7	4
101	Value of MRI in evaluating urachal carcinoma: A single center retrospective study. Urologic Oncology: Seminars and Original Investigations, 2022, 40, 345.e9-345.e17.	0.8	4
102	An unsuspected MR projectile: A "wooden―chair with metal bracing. Journal of Magnetic Resonance Imaging, 2006, 23, 781-782.	1.9	3
103	Reply: Breast Cancer Staging: To Which Women Should 18F-FDG PET/CT Be Offered?. Journal of Nuclear Medicine, 2015, 56, 1293.2-1294.	2.8	3
104	David Versus the Goliaths for the Detection of Bone Metastases. Journal of Nuclear Medicine, 2017, 58, 1776-1777.	2.8	3
105	Mazabraud's Syndrome Mimicking Metastases on FDG PET/CT in a Patient With Colon Cancer. Clinical Nuclear Medicine, 2018, 43, 625-626.	0.7	3
106	Intra-arterial Melphalan for Neurologic Non-Langerhans Cell Histiocytosis. Neurology, 2021, 96, 1091-1093.	1.5	3
107	FDG-PET/CT versus contrast enhanced CT for prediction of progression-free and disease-specific survival in stage IV breast cancer patients Journal of Clinical Oncology, 2015, 33, 1051-1051.	0.8	3
108	FDG-Avid Intrathecal Inflammation Following Administration of Intrathecal Methotrexate. Clinical Nuclear Medicine, 2016, 41, 995-997.	0.7	2

#	Article	IF	CITATIONS
109	FDG-Avid Venous Malformation Could Mimic Malignancy on 18F-FDG PET/CT. Clinical Nuclear Medicine, 2013, 38, 826-828.	0.7	1
110	Adalimumab-Induced Epstein-Barr Virus–Related Lymphoproliferative Disorder on FDG PET/CT. Clinical Nuclear Medicine, 2018, 43, 344-345.	0.7	1
111	Patient Repositioning Reveals a Malignant Pleura Effusion Initially Mistaken as a Bone Metastasis on 18FDG PET/CT. Clinical Nuclear Medicine, 2019, 44, 969-970.	0.7	1
112	The QIBA Profile for FDG PET/CT: Improving the Value of PET. Radiology, 2020, 294, 658-659.	3.6	1
113	Extramedullary Myeloma of the Uterus on 18F-FDG PET/CT. Clinical Nuclear Medicine, 2020, 45, 873-875.	0.7	1
114	Hill-Sachs Lesion on FDG PET/CT. Clinical Nuclear Medicine, 2013, 38, 65-66.	0.7	0
115	Focused Regional FDG PET/CT Detects More Osseous Metastases Than Does Whole-Body PET/CT. Clinical Nuclear Medicine, 2013, 38, 217-218.	0.7	0
116	"Comment on Hatzoglou et al.: Dynamic contrast-enhanced MRI perfusion vs 18FDG PET/CT in differentiating brain tumor progression from radiation injury―Reply. Neuro-Oncology, 2017, 19, now286.	0.6	0
117	Transient Osteoporosis of the Hip on FDG PET/CT. Clinical Nuclear Medicine, 2017, 42, 401-402.	0.7	0
118	Skeleton on FDG PET/CT. , 2019, , 9-32.		0
119	Lymph Nodes on FDG PET/CT. , 2019, , 211-223.		0
120	Spleen on FDG PET/CT. , 2019, , 127-131.		0
121	Acute Aortic Dissection Initially Suspected on 18F-FDG PET/CT. Clinical Nuclear Medicine, 2020, 45, 819-820.	0.7	0
122	Malignant perivascular epithelioid cell tumor of the ileum on 18F-fluorodeoxyglucose positron emission tomography/computed tomography with pathological correlation. World Journal of Nuclear Medicine, 2021, 20, 208.	0.3	0